

Orientation control by flow: Exact results and Langevin simulations

C. Tannous

Laboratoire de Magnétisme de Bretagne CNRS-FRE 3117,
Université de Bretagne Occidentale, 29285 Brest, France.

(Dated: April 2008)

Rod shaped objects suspended in a flowing liquid might be orientated by the velocity, nature of the liquid, the flow and the geometry of the channel containing the flow. Orientation settings might enhance or inhibit certain chemical reactions between the objects, other chemicals or with the walls of vessels holding the flowing suspension. The probability density function (PDF) describing the orientations of rod shaped objects in a flowing liquid satisfies a Fokker-Planck equation whose solution is obtained analytically as well as numerically from Langevin simulations for different flow parameters. The analytical and numerical methods developed in the present work enable us to calculate accurately the PDF for a range of the Peclet number α covering several orders of magnitude, $10^{-4} \leq \alpha \leq 10^8$. We apply these results to the experimental determination of dichroism and birefringence of the suspension as a function of α .

Keywords: Flows in ducts, Diffusion. Simulation, Stochastic analysis

PACS numbers: 47.60.+i, 66.10.Cb, 87.53.Vb, 05.10.Gg

I. INTRODUCTION

In many physical, chemical, biological processes, the behavior and orientation of rod shaped objects (RSO) such as fibers, nanotubes, nanowires, DNA, macromolecules... suspended in a flowing liquid affect the transport, rheology, chemical and hydrodynamic characteristics of the suspension [1]. Orientation control for the sake of aligning or separating RSO, enhancing reaction between them, with other chemicals or vessel walls is important in many areas of science and technology such as sedimentation, blood flow, pulp and paper, polymer processing, microfluidic devices, ferrofluids...

Objects suspended in flow undergo two types of motion: smooth motion due to the average fluid velocity field and erratic random motion produced by the fluctuating fluid velocity, temperature and inertia driven motion. The resulting change in the suspension microstructure can have a significant effect on the mechanical, thermal, optical, electrical, magnetic and chemical properties.

The objective of this work is to investigate the effect of non-turbulent flow on the rotational diffusion of a dilute suspension of non-interacting RSO in a planar contraction and how its impact might be measured with an optical measurement such as dichroism or birefringence of the suspension.

Generally a Fokker-Planck equation accurately models the orientation state of non-interacting RSO in hydrodynamic nonhomogenous flow and the main orientation parameter is the rotational Peclet number α that represents the interplay between the randomizing effect of temperature induced rotational diffusion and the orienting effect of streamwise mean rate of strain due to the flow [2].

Two types of flow are of particular importance: simple shear flow and elongational (or, extensional) flow. Simple shear flow is a velocity profile where the gradient in the

fluid flow velocity is constant, whereas for elongational flow the sample is compressed in one direction and elongated in the other direction. Such flows can be either stationary or oscillatory.

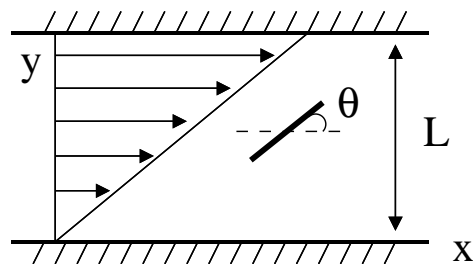


FIG. 1: Geometry of the shear flow and the RSO of length ℓ making an angle θ with the flow direction along x . The shear rate of the flow is $\dot{\gamma} = \frac{\partial v_x}{\partial y}$.

The rotational Peclet number measuring the relative strength of hydrodynamic interactions and Brownian forces is defined mathematically as the ratio of hydrodynamic shear flow and rotational diffusion constant:

$$\alpha = \frac{\dot{\gamma}}{D_{rot}} \quad (1)$$

where $\dot{\gamma}$ is the hydrodynamic shear rate and D_{rot} the thermal diffusion [3].

The flow shear rate defined by $\dot{\gamma} = \frac{\partial v_x}{\partial y}$ with v_x the velocity field in the x direction of the flow (see fig. 1) is related to translational degrees of freedom whereas D_{rot} , the Brownian diffusion coefficient, governs the rotational motion of the RSO around its center of mass and hence relates to rotational degrees of freedom.

The rotational diffusion coefficient, D_{rot} is given by [4]:

$$D_{rot} = \frac{3k_B T}{\pi \eta_s \ell^3} \left[\ln\left(\frac{\ell}{d}\right) - 0.8 \right] \quad (2)$$

with k_B the Boltzmann constant, T the temperature, expresses the influence of flow on orientation. Usually it is determined experimentally from RSO orientation studies in a constriction with flat walls. ℓ is the RSO length d its diameter and η_s the solvent viscosity.

Non-interacting dilute concentration of RSO of density ρ , yield the conditions: $\rho\ell^2d < 1$ and $\rho\ell^3 < 1$.

The Reynolds number defined as [5]: $Re = \frac{\rho_s \dot{\gamma} L^2}{\eta_s}$ is much smaller than 2000 in order to have a non-turbulent flow. ρ_s is solvent density and L the width of the planar contraction (see fig. 1).

Boeder [6] is the first to have studied this problem in the bulk of a flowing liquid from the theoretical point of view. He derived, without the use of the Langevin formalism or the Fokker-Planck equation [7], an ordinary differential equation (ODE) governing the PDF $P(\theta)$ describing the average orientations of the RSO:

$$\frac{d^2}{d\theta^2}P(\theta) + \frac{d}{d\theta}[\alpha \sin^2(\theta)P(\theta)] = 0 \quad (3)$$

The above ODE is derived for the motion of RSO, of negligible cross-sectional area, in the plane of the flow, without any boundary conditions and in the dilute case. The angle θ describes the orientations of the RSO with respect to the liquid flow direction (see fig. 1).

Since the PDF $P(\theta)$ is π -periodic one might write a Fourier series solution valid for small and large values of α . For small values of α we perform a perturbation analysis of the Fourier series whereas for large values of α asymptotic analysis might be done [6]. Many improvements have been made since, to remove restrictions on the cross-sectional areas of the RSO, consider rotational diffusion in three dimensions and introduce internal vibrational and rotational degrees of freedom within the RSO.

The purpose of this work is to provide a solution in closed form for the above ODE with different analytical and numerical methods to obtain $P(\theta)$ for a wide range of the Peclet number α and gauge the impact on orientation control and the measurable optical properties. Another goal is to compare the analytical approach with Langevin simulations of the PDF, under the same conditions in the bulk of a flowing liquid. This comparison is useful because it can confirm on one hand the robustness of the analytical methods. On the other hand it provides a necessary limiting bulk condition for similar simulations near solid surfaces.

This paper is organised as follows: In Section II, we present an exact analysis of the ODE (see eq. 3) to obtain the probability distribution function (PDF), for a wide range of α . In Section III, Langevin simulation and comparison with the exact results are presented. In section IV, large values of α are treated along with scaling results, optical properties and flow control. The conclusions are given in Section V.

II. ANALYTICAL SOLUTION

In this section, a procedure for the accurate numerical analysis of the ODE (see eq. 3) and its associated probability distribution function, $P(\theta)$, is given for a wide range of α . Turbulence effects are known to take place for large values of α (typically for $\alpha \geq 10^4$). Although the above ODE (eq. 3) ceases to apply beyond this limit, the present mathematical analysis is not limited by this, and numerical solutions may be calculated in our approach for values of $\alpha \sim 10^8$. $P(\theta)$ is the solution of a second-order ODE (eq. 3). The PDF is π -periodic since the RSO are indistinguishable when oriented at θ or $\theta + \pi$; hence the π -periodic boundary conditions:

$$P(0) = P(\pi) \text{ and } P'(0) = P'(\pi) \quad (4)$$

where $P'(\theta) = \frac{d}{d\theta}P(\theta)$. Moreover, the PDF has to be normalised over the interval $[0, \pi]$:

$$\int_0^\pi P(\theta)d\theta = 1 \quad (5)$$

The determination of the associated PDF is consequently a constrained (because of the normalization condition) boundary value problem (BVP) eq. 3. Nevertheless one may derive two other versions of the ODE eq. 3. The first is a 1D equation that takes the form:

$$P'(\theta) + \alpha \sin^2(\theta)P(\theta) = C \quad (6)$$

with initial condition: $P(\theta = 0) = P(0)$. This is mathematically sound provided the initial value $P(0)$ and the constant C are known as shown below. The second form is a 2D system that may be presented as:

$$\begin{cases} \frac{d}{d\theta}P(\theta) = P'(\theta) \\ \frac{d}{d\theta}P'(\theta) = -\alpha \sin(\theta)[\sin(\theta)P'(\theta) + 2 \cos(\theta)P(\theta)] \end{cases} \quad (7)$$

Several technical procedures may be used to determine $P(\theta)$, depending on the different possible formulations of the problem, as an initial value problem (eq. 6 and eq. 7) or as a BVP (eq. 4). In all cases two quantities, the constant C in eq. 6 (equal to $P'(0)$ by substituting $\theta = 0$ and assuming finiteness of $P(\theta \rightarrow 0)$ in eq. 6) and the initial value $P(0)$, have to be evaluated for any value of α . We have developed two methods, described below, to determine C and $P(0)$. Firstly, a direct method based on the solution of eq. 6, and secondly a minimisation method based on a multidimensional secant method (also called Brodyden method [8]).

The direct method to evaluate C and $P(0)$ is as follows. The formal solution of eq. 6 may be given generally as:

$$P(\theta) = C \exp[\alpha[\sin(2\theta)/2 - \theta]/2] \times \int_{-\infty}^{\theta} \exp[-\alpha(\sin(2x)/2 - x)/2] dx \quad (8)$$

The lower limit $-\infty$ is surprising since the problem is defined over the angular interval $[0, \pi]$. It can analytically be shown that the lower limit $-\infty$ is the only possibility compatible with the boundary conditions given by eq. 4. Performing a change of variables, the solution may then be written as:

$$P(\theta) = (2C/\alpha) \exp[\alpha \sin(2\theta)/4] \times \int_0^{\infty} \exp(-x) \exp[\alpha \sin(4x/\alpha - 2\theta)/4] dx \quad (9)$$

The form in eq. 10 is more stable numerically than the previous one of eq. 9, since the numerically troublesome $\exp(\theta)$ and $\exp(-\theta)$ terms are avoided. Nevertheless when α increases the $\exp[\alpha \sin(2\theta)/4]$ term will cause problems despite the bounded values of the sine function, forcing us to turn to other methods based on extrapolation techniques. The constant C is next determined from the normalisation condition of the PDF (eq. 5) yielding:

$$C = \frac{(\frac{\alpha}{2})}{\int_{-\frac{\pi}{2}}^{\frac{\pi}{2}} d\theta \int_0^{\infty} dx \exp(-x) \exp[(\frac{\alpha}{2}) \sin(\frac{2x}{\alpha}) \cos(2\theta - \frac{2x}{\alpha})]} \quad (10)$$

whereas $P(0)$ is given by

$$P(0) = (2C/\alpha) \int_0^{\infty} \exp(-x) \exp[\alpha \sin(4x/\alpha)/4] dx \quad (11)$$

The PDF depends on α which we may want to vary over several orders of magnitude. The difficulty in solving the ODE stems from the fact that its nature may be modified when α increases, turning the problem into a singular perturbation one in α^{-1} as detailed in section IV.

III. LANGEVIN SIMULATIONS AND COMPARISON WITH THE EXACT EQUATION

We convert the deterministic equation of motion for the RSO into a Langevin equation by adding a random force term and analyze statistically the resulting equation.

We start from the angular speed:

$$\frac{d\theta}{dt} = \omega = -\dot{\gamma} \sin^2(\theta) \quad (12)$$

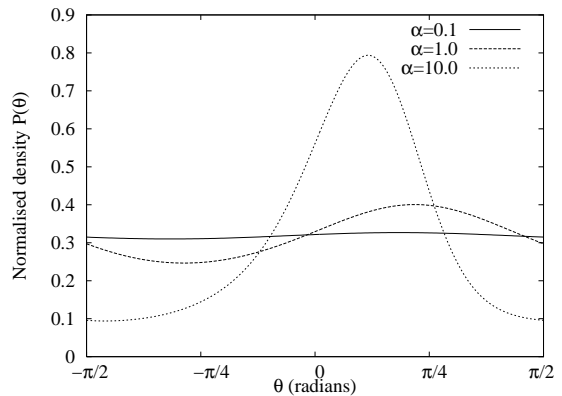


FIG. 2: Analytical PDF as a function of θ for small $\alpha=0.1$, 1, and 10.0 normalised over the interval $[-\pi/2, \pi/2]$

and add to it a random term $\lambda\xi(t)$ with White noise statistical properties:

$$\langle \xi(t) \rangle = 0 \text{ and } \langle \xi(t)\xi(t') \rangle = \delta(t - t') \quad (13)$$

This means the hydrodynamic forces tend to act on the RSO rotating them in the shear flow with an average angular speed ω in the presence of perturbing fast random orientations represented by $\xi(t)$. The equation of motion for θ becomes:

$$d\theta = -\dot{\gamma} \sin^2(\theta) dt + \lambda dW(t) \quad (14)$$

where $dW(t) = \xi(t)dt$ is a Wiener process [7].

This is an Itô Stochastic Differential Equation (SDE) (see for instance Gardiner [7]) that can be transformed into a 1D Fokker-Planck equation that will be identified with the ODE equation 3.

A single stochastic variable θ Itô SDE [7] of the form:

$$d\theta = A(\theta, t)dt + \sqrt{B(\theta, t)}dW(t) \quad (15)$$

is equivalent to a 1D Fokker-Planck equation:

$$-\frac{d}{d\theta}[A(\theta)P(\theta)] + \frac{1}{2} \frac{d^2}{d\theta^2}[B(\theta)P(\theta)] = 0 \quad (16)$$

Identification with the ODE equation 3 yields the value of the coefficient $A(\theta)$ as: $A(\theta) = -\frac{1}{2}B\alpha \sin^2(\theta)$ whereas B is a constant independant of θ . Hence the SDE writes:

$$d\theta = -\frac{1}{2}B\alpha \sin^2(\theta)dt + \sqrt{B}dW(t) \quad (17)$$

The hydrodynamic forces tend to act on the RSO rotating them in the shear flow with an average angular speed ω , given by eq. refangspeed.

This completely characterizes the SDE parameters as:

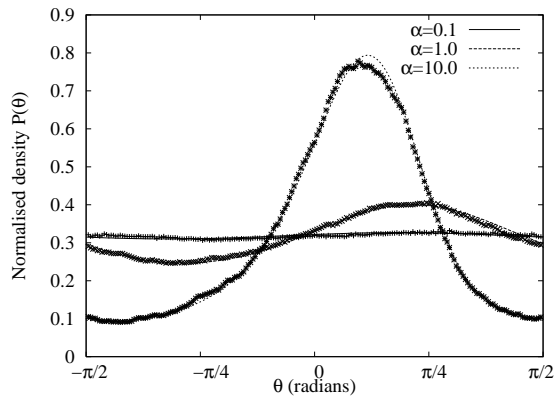


FIG. 3: Langevin simulated PDF as a function of θ for small $\alpha=0.1, 1.$ and 10.0 normalised over the interval $[-\pi/2, \pi/2]$. The analytical curves are displayed for comparison.

$$\dot{\gamma} = \frac{1}{2}B\alpha, \quad B = 2D_{rot} \quad (18)$$

The method of integration we use, is a 4th order Stochastic Runge-Kutta routine: 3O-3S-2G developed by Helfand [9] where 3O is third order, 3S is three stages 2G means we need two Gaussian Random Variables per step. Order k means the solution agrees with the average Taylor expansion [10] of the series solution to order h^k where h is the integration step.

In order to assess the validity of the method, we ran several tests and compared the results to known analytical solutions.

The results we find for the Langevin simulated PDF are displayed in fig. 3 and fig. 5 for small and large values of the Peclet number. The results of the Langevin simulation converged after $\sim 10^7$ steps toward the analytically determined PDF.

IV. LARGE VALUES OF THE PECLET NUMBER: SCALING AND OPTICAL PROPERTIES

In order to cope with the wide range over which α may vary, we classify the various methods for solving the problem according to the value of α .

For moderate α in the range : $[10^{-4}, 10^2]$, we can proceed either directly from the analytic solution of the first-order ODE or once C and $P(0)$ are known, a simple 1D Runge-Kutta method is used to solve the first-order ODE.

In order to find C and $P(0)$ by a minimisation method based on a multidimensional secant (Broyden method), and a 2D Runge-Kutta integration method to solve the two first-order ODE system (Eqs. 7). We have the following two conditions:

$$\begin{aligned} & \text{minimum } |P(0) - P(\pi)|; \\ & \text{minimum } \left| \int_0^\pi P(\theta)d\theta - 1 \right| \end{aligned} \quad (19)$$

In the above minimisation problem, the first condition comes from periodicity of the PDF, whereas the second expresses the normalisation of the PDF.

When α becomes large i.e. in the range : $[10^2, 10^5]$, we calculate C and $P(0)$ by an extrapolation method and solve eq. 6, or the system 7, with singular perturbation integration methods [8]. To illustrate the different numerical methods used in our approach to solve the Boeder differential equation, and to calculate the PDF, some numerical results are presented, for a wide range of values of α . In Figs. 2 and 4, these PDF functions are depicted, for moderate ($\alpha=0.1, 1, 10.$) and large values ($\alpha=100., 1000.$ and $10,000$) of α . The PDF results are normalised with respect to unity. The scaling results are presented next for large values of α .

A. Scaling results

Eq. 10 can be simplified for large α by replacing the cosine term in the exponential integrand by 1, since it will lead to higher order terms in $1/\alpha$ and reducing the double integration appearing in the C denominator into a simpler one, namely:

$$C = \frac{\alpha^{\frac{1}{3}}}{[2\theta_{max} \int_0^\infty \exp(-2x^3/3)dx]} \quad (20)$$

where θ_{max} is the value of the angle that corresponds to the PDF maximum at which the ODE eq. 3 writes:

$$\alpha \sin^2(\theta_{max})P(\theta_{max}) = C \quad (21)$$

Using the definite integral [11]:

$$\int_0^\infty x^{\nu-1} \exp(-\mu x^p)dx = \frac{1}{p} \mu^{-\frac{\nu}{p}} \Gamma\left(\frac{\nu}{p}\right) \quad (22)$$

we get:

$$C = \frac{3\alpha^{\frac{1}{3}}}{\left[2\theta_{max}\left(\frac{2}{3}\right)^{-\frac{1}{3}}\Gamma\left(\frac{1}{3}\right)\right]} \quad (23)$$

Similarly the argument of the exponential integrand in eq. 11, yields

$$\begin{aligned} P(0) &= (2C/\alpha^{\frac{1}{3}}) \int_0^\infty \exp(-8x^3/3\alpha^2)dx \\ &= (2C/3\alpha^{\frac{1}{3}}) \left(\frac{8}{3}\right)^{-\frac{1}{3}} \Gamma\left(\frac{1}{3}\right) \end{aligned} \quad (24)$$

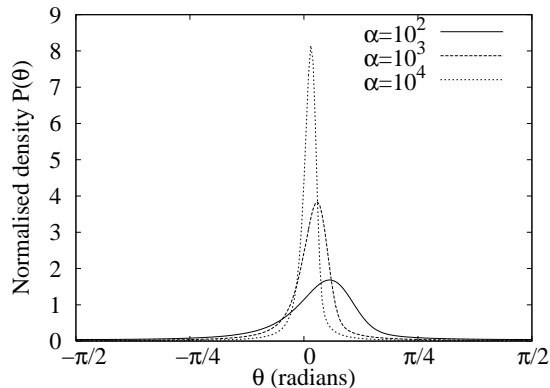


FIG. 4: Analytical PDF as a function of θ for large $\alpha=100.0$, 1000. and 10,000. normalised over the interval $[-\pi/2, \pi/2]$

The normalisation of the PDF in Eq. 5 when α is large, yields after using eq. 21:

$$\theta_{max}P(\theta_{max}) \sim \text{constant} \quad (25)$$

which is the area under the PDF curve since the distribution function becoming sharply peaked around θ_{max} , leads to a PDF approximately triangular in shape with a height $P(\theta_{max})$ and a base equal to $2\theta_{max}$. Hence, we obtain the following leading behaviours:

$$\begin{aligned} P(0) &\sim \alpha^{1/3}, \quad C \sim \alpha^{2/3}; \\ \theta_{max} &\sim \alpha^{-1/3}, \quad P(\theta_{max}) \sim \alpha^{1/3} \end{aligned} \quad (26)$$

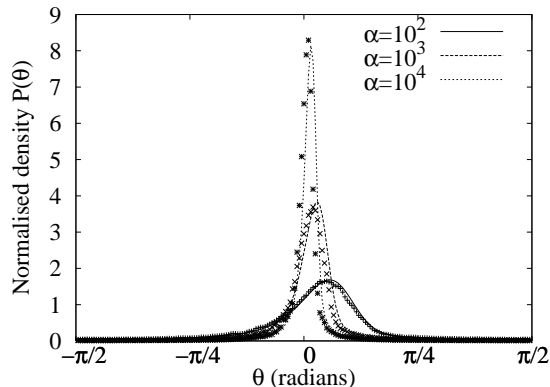


FIG. 5: Langevin simulated PDF as a function of θ for large $\alpha=100.0$, 1000. and 10,000. normalised over the interval $[-\pi/2, \pi/2]$. The analytical curves are displayed for comparison.

The exponents controlling the asymptotic behaviour above are all consistent with respect to each other, besides we have checked them numerically up to quite large values of $\alpha \leq 10^8$.

Recently, Fry et al. [12] made optical studies of Carbon nanotube suspensions in polyisobutylene and aqueous single-stranded DNA solutions and were able to show

that shear-induced birefringence and dichroism (SABD) $\Delta n'$, $\Delta n''$ are both proportional to a single quantity $S = \langle P_2(\cos \theta) \rangle$ so-called nematic order parameter that is zero for an isotropic distribution of orientations and 1 for perfect alignment. $P_2(\cos \theta)$ is the Legendre polynomial of order 2 and $\Delta n'$ is extracted from the phase difference between the transmitted and reference signal whereas $\Delta n''$ is extracted from the attenuation of light intensity.

They found that SABD scale as $\alpha^{0.16}$ for values of the Peclet number as large as 10^{10} as they approach the saturation value of 1.

Therefore we set out to analyse the scaling of S in the Boeder case. Our results shown in fig. 6 indicate that in our case, the SABD saturate to 1 and that might be attributed to the following argument.

As the Peclet number increases the orientational PDF becomes sharply peaked around θ_{max} that scales as $\alpha^{1/3}$. Since, it is required that the PDF should be normalised we ought to have the value of S behaving as:

$$\begin{aligned} S &= \int_{-\pi/2}^{\pi/2} P(\theta)P_2(\cos \theta)d\theta \\ &\sim \int_{-\theta_{max}}^{\theta_{max}} P(\theta)P_2(\cos \theta)d\theta \\ &\sim 2\theta_{max}P(\theta_{max})P_2(\cos \theta_{max}) \end{aligned} \quad (27)$$

That implies, given eq. 25, that S behaves as $P_2(\cos \theta_{max}) = \frac{1}{2}(3 \cos^2 \theta_{max} - 1) \sim 1 - \frac{3}{2}\alpha^{-2/3}$ close to the behaviour found in fig. 6 and obtained from full numerical integration.

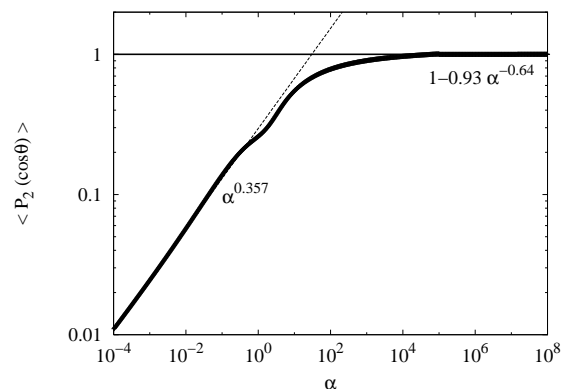


FIG. 6: Average value of $P_2(\cos \theta)$ versus Peclet number α displaying the scaling behaviour at large values of α as it is approaching 1. The power law behaviour $\sim \alpha^{0.357}$ for small values of α (straight dotted lines) and $\sim 1 - 0.93\alpha^{-0.64}$ for large values of α are indicated.

Since θ_{max} is a measure of the standard deviation (for large values of α) in the fluctuations of the angle θ about the flow main direction, the RSO orientation controllability with flow can be analysed with the variation of the angle θ_{max} with the Peclet number α . Increasing α makes

the orientational PDF more sharply peaked around θ_{max} and with the requirement that the PDF should be normalised, θ_{max} approaches the standard deviation.

In fig. 7 the variation of θ_{max} with the Peclet number α is depicted implying that orientation controllability is achieved when θ_{max} drops below a small specified value. For instance, one has to have $\alpha \sim 400$ in order to achieve $\theta_{max} \leq 0.1$ radian (see fig. 7) whereas $\alpha \sim 6 \times 10^5$ is required in order to have $\theta_{max} \leq 0.01$ radian.

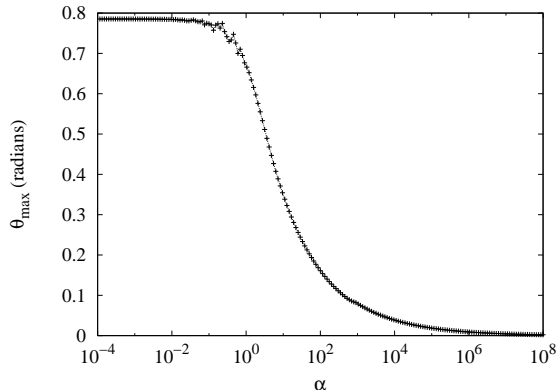


FIG. 7: Variation of the angle θ_{max} (in radians) with the Peclet number α . For small values of α , θ_{max} saturates at a value of about 0.8 radian that is close to $\frac{\pi}{4}$ as seen in fig. 2. When α is increased beyond several 100, θ_{max} drops to small values indicating that orientation control has set in.

V. CONCLUSIONS

The PDF describing the average orientations of RSO in a flowing liquid is analytically determined and accurately evaluated as a function of α , the rotational Peclet number over a wide range. The impact of α on orientation control and optical properties is examined. Special analytical as well as numerical methods are developed and presented in order to calculate accurately this PDF for a wide range of α over the interval $[10^{-4} - 10^8]$. Langevin simulations agree well with the numerical solutions of the PDF in the bulk of the flowing liquid for arbitrary values of α and confirm the validity of the analytical solution. Scaling results (valid for $\alpha \geq 10^3$) are also presented. The mathematical nature of the ordinary differential equation that the PDF should satisfy is revealed as a singular perturbation problem when α^{-1} becomes smaller than about 10^{-3} and special numerical techniques [8] ought to be used in order to evaluate the PDF and related physical quantities.

The analytical approach, Langevin simulation and scaling results should be considered equally as complementary tools for this type of study and as a valuable guide to the harder cases where we have either turbulent flow, presence of RSO internal degrees of freedom or more complex flow geometries.

Acknowledgements

The author would like to thank M. Aoun for his help in the statistical analysis of the simulation results.

-
- [1] R.B. Bird, C.F. Curtiss, R.C. Armstrong, O. Hassager, *Dynamics of Polymeric Liquids*, vols. 1 and 2, Wiley, New York (1987).
 - [2] M. Parsheh, M. L. Brown, C. K. Aidun, J. Non-Newtonian Fluid Mechanics, **136**, 38 (2006).
 - [3] F. Reif, *Statistical and Thermal Physics*, McGraw-Hill, New-York (1985).
 - [4] M. Doi, S.F. Edwards, *The Theory of Polymer Dynamics*, Clarendon Press, Oxford (1986).
 - [5] L. D. Landau and E. M. Lifshitz, *Fluid Mechanics*, Pergamon, Oxford (1975).
 - [6] P. Boeder, Z. Physik **75**, 258 (1932).
 - [7] C. W. Gardiner, *Handbook of Stochastic Methods*, 2nd ed. (Springer-Verlag, Berlin, 1990).
 - [8] W. H. Press, W. T. Vetterling, S. A. Teukolsky and B. P. Flannery, *Numerical Recipes in C: The Art of Scientific Computing* Second Edition, Cambridge University Press, New-York (1992).
 - [9] E. Helfand, Bell System Tech. J. **58**, 2289 (1979).
 - [10] A. Greiner, W. Strittmatter and J. Honerkamp, J. Stat. Phys. **51**, 95 (1988).
 - [11] I. S. Gradshteyn and I. M. Ryzhik, *Table of Integrals, Series and Products*, 3.478, Academic Press, New-York (1980).
 - [12] D. Fry, B Langhorst, H. Wang, M. L. Becker, B.J. Bauer, E.A. Grulke and E.K. Hobbie, J. Chem. Phys. **124**, 054703 (2006).